CHAPTER 5

RESPONSE OF DEFLECTION AND THERMAL MOMENT OF TIMOSHENKO MICROBEAMS CONSIDERING MODIFIED COUPLE STRESS THEORY AND DUAL-PHASE-LAG HEAT CONDUCTION MODEL

5.1 Introduction[1]

The present chapter focuses on the vibration analysis of Timoshenko microbeams considering modified couple stress theory (MCST) in the context of generalized dual-phase-lag (DPL) thermoelastic heat conduction model. It is worth mentioning here that previous chapters are based on the study of Euler-Bernoulli micro and nanobeams that are more useful for small deflection only, while Timoshenko microbeams are applicable for small deflection as well as for large deflection.

The study of Taati et al. (2014a) provided the inspiration for the present work. They developed an explicit formulation for coupled thermoelasticity addressing a Timoshenko microbeam in their study using MCST and non-Fourier heat conduction equation with one relaxation time. They found that by applying the non-Fourier model, the prediction of deflection under MCST is larger in comparison of classical theory. Further, this work has been extended considering the strain gradient thermoelasticity theory by Taati et

[1]The content of this chapter is published in ***Composite Structures***, 263 (2021):113620.

al. (2014b) in order to capture size effect in Timoshenko microbeam. Awrejcewicz et al. (2020) introduced Timoshenko beam model carrying functionally graded properties along with their thickness taking size-dependency into account. Recently, Kumar (2020) derived the expressions for thermal moment and deflection of a Timoshenko beam considering MCST and non-Fourier heat conduction model with three relaxation times.

According to the literature, no research has been done so far on the vibration response of Timoshenko microbeams using MCST and DPL thermoelastic model. The current work aims to fulfill this gap. The explicit expressions for normalized midspan deflection and thermal moment of a Timoshenko microbeam considering MCST and DPL heat conduction model are derived. The constructed mathematical model is capable for predicting the size-effects in microbeam due to the presence of the internal material length-scale parameter. The governing equations and related boundary conditions of microbeam are constructed by employing the Hamilton's principle. The DPL heat conduction theory takes into account the microscopic effects in the heat transfer process and involves the concepts of two phase-lags in the constitutive relation of temperature gradient and heat flux. It is therefore attempted to understand the impact of two phase-lags on vibrations of a Timoshenko beam considering MCST. The obtained results in the present context are compared to the corresponding results obtained in the contexts of other existing models like the Lord-Shulman (LS) and classical Fourier heat conduction models. Analytical results are illustrated by carrying out computational work for a Timoshenko microbeam made of Silicon material at the constant reference temperature. It is investigated that the present results agree with the results under LS and Fourier heat conduction models for small-time range while they differ significantly as time increases. The present results also show a strong influence of phase-lags time parameters on the variation of deflection and thermal moment of the microbeam. A prominent difference in the results for MCST in comparison to the classical continuum theory is indicated when we employ the DPL heat conduction theory.

5.2 Problem formulation

5.2.1 Governing equations for Timoshenko microbeam

We consider a Timoshenko beam model to describe the microbeam deformation behavior. On the basis of the Timoshenko beam model, the components of the infinitesimal displacement field can be expressed in the form (Taati et al., 2014)

$$u_x = u\left(x,t\right) + z\Theta_x\left(x,t\right), \quad u_y = 0, \quad u_z = w\left(x,t\right) \tag{5.2.1}$$

where $u\left(x,t\right)$ is the in-plane displacement of the particles on the mid-plane. $\Theta_x\left(x,t\right)$ represents the rotational angle of cross-section of the beam about $y-$axis. t and z respectively denote the time and the distance of a point from mid-plane.

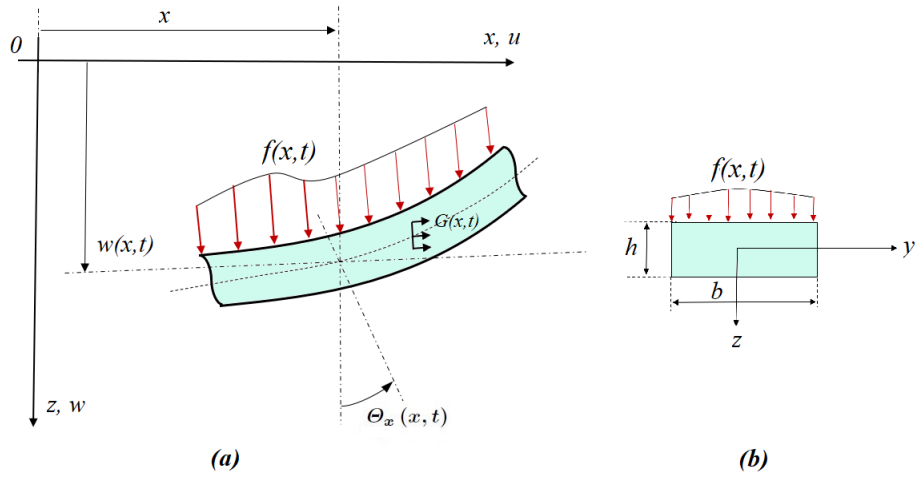

Figure 5.2.1: Geometry of Timoshenko microbeam (a) loading and the introduced coordinate system (b) cross-section of microbeam.

Substituting Eq. (5.2.1) into Eq. (3.2.2) gives

$$\epsilon_{xx} = \frac{\partial u}{\partial x} + z\frac{\partial \Theta_x}{\partial x}, \quad \epsilon_{xz} = \epsilon_{zx} = \frac{1}{2}\left(\Theta_x + \frac{\partial w}{\partial x}\right), \quad \epsilon_{yy} = \epsilon_{zz} = 0 \tag{5.2.2}$$

The volumetric strain tensor is given by

$$\epsilon = \epsilon_{xx} + \epsilon_{yy} + \epsilon_{zz} = \frac{\partial u}{\partial x} + z\frac{\partial \Theta_x}{\partial x} \tag{5.2.3}$$

The non-zero components of rotation vector and symmetrical part of curvature tensor can be found as:

$$\vartheta_x = \vartheta_y = \frac{1}{2}\left(\Theta_x - \frac{\partial w}{\partial x}\right) \tag{5.2.4}$$

$$\chi_{xy} = \chi_{yx} = \frac{1}{4}\left(\frac{\partial \Theta_x}{\partial x} - \frac{\partial^2 w}{\partial x^2}\right) \tag{5.2.5}$$

From Eqs. (3.2.5) and (3.2.6), the non-zero components of stress and couple stress tensors become

$$\sigma_{xx} = E\left(\frac{\partial u}{\partial x} + z\frac{\partial \Theta_x}{\partial x}\right) - \beta\theta, \quad \sigma_{xz} = \sigma_{zx} = \mu\left(\Theta_x + \frac{\partial w}{\partial x}\right) \tag{5.2.6}$$

$$m_{xy} = m_{yx} = \frac{1}{2}\mu l^2\left(\frac{\partial \Theta_x}{\partial x} - \frac{\partial^2 w}{\partial x^2}\right) \tag{5.2.7}$$

Using Eqs. (5.2.2)-(5.2.5), (5.2.6), and (5.2.7) into Eq. (3.2.1), the strain energy is obtained in the following form:

$$U = \frac{1}{2}\int_0^L \int_A \left[E\left(\frac{\partial u}{\partial x} + z\frac{\partial \Theta_x}{\partial x}\right)^2 - (\beta\theta)\left(\frac{\partial u}{\partial x} + z\frac{\partial \Theta_x}{\partial x}\right) + \mu\left(\Theta_x + \frac{\partial w}{\partial x}\right)^2 + \left(\frac{1}{2}\mu l^2\right)\left(\frac{\partial \Theta_x}{\partial x} - \frac{\partial^2 w}{\partial x^2}\right)^2\right] dAdx \tag{5.2.8}$$

The kinetic energy can be expressed as:

$$\begin{aligned} K =& \frac{1}{2}\int_V \rho\left[\left(\frac{\partial u_x}{\partial t}\right)^2 + \left(\frac{\partial u_y}{\partial t}\right)^2 + \left(\frac{\partial u_z}{\partial t}\right)^2\right] dV \\ =& \frac{1}{2}\int_0^L \int_A \rho\left[\left(\frac{\partial u}{\partial t} + z\frac{\partial \Theta_x}{\partial t}\right)^2 + \left(\frac{\partial w}{\partial t}\right)^2\right] dAdx \end{aligned} \tag{5.2.9}$$

where ρ symbolizes the density of mass. The moment of inertia (I) and the resultants

of thermal moments (M_T) and (N_T) are given by

$$I = \int_A z^2 dA = \frac{bh^3}{12} \tag{5.2.10}$$

$$M_T = \int_A \beta\theta z dA = b\int_{-h/2}^{+h/2} \beta\theta z dz \tag{5.2.11}$$

$$N_T = \int_A \beta\theta dA = b\int_{-h/2}^{+h/2} \beta\theta dz \tag{5.2.12}$$

The work done caused by the external loads $f\left(x,,t\right)$ applied on the beam can be written as:

$$W = \int_0^L \left[f\left(x,t\right)w\left(x,t\right) + G\left(x,t\right)u\left(x,t\right)\right]dx + \left[\widetilde{N}u\left(x,t\right) + \widetilde{V}w\left(x,t\right) + \widetilde{M}\Theta_x + \widetilde{V_h}\left(\frac{\partial w}{\partial x}\right)\right]_{x=0}^{x=L} \tag{5.2.13}$$

The term $\widetilde{N}$ represents the resultant axial force and $\widetilde{V}$ represents transverse force caused by the components of classical stress acting on the beam's section. These two forces $\widetilde{N}$ and $\widetilde{V}$ are the works that are conjugated to u and w, respectively. The term $\widetilde{M}$ is used to denote the resultant moment in a section caused by components of classical stress which is work conjugate to Θ_x. The notations $\widetilde{V_h}$ and $\widetilde{M_h}$ stand for the higher order resultant moment in a section caused by the higher order stresses applied on the section which are the work conjugate to $\frac{\partial w}{\partial x}$ and Θ_x, respectively.

The governing equations of motion of microbeam including thermal effects are formulated with the help of Hamilton's principle. The Hamilton's principle on the time interval t_1 and t_2 gives

$$\delta\int_{t_1}^{t_2}\left(K - U + W\right)dt = 0 \tag{5.2.14}$$

The operator δ denotes here the variation. Inserting Eqs. (5.2.8), (5.2.9), and (5.2.13) into Eq. (5.2.14) and making the assumption that the variations of $\delta u, \delta w$, and $\delta\Theta_x$ at

time t_1 and t_2 are zero, the governing equations of motion can be given by

$$\delta u : (-EA)\left(\frac{\partial^2 u}{\partial x^2}\right) + \frac{1}{2}\left(\frac{\partial N_T}{\partial x}\right) = -\rho A\left(\frac{\partial^2 u}{\partial t^2}\right) + G\left(x,t\right) \tag{5.2.15}$$

$$\delta\Theta_x : -\left[(EI) + \left(\frac{\mu A l^2}{4}\right)\right]\left(\frac{\partial^2 \Theta_x}{\partial x^2}\right) + (\mu A)\left(\Theta_x + \frac{\partial w}{\partial x}\right) + \left(\frac{\mu A l^2}{4}\right)\left(\frac{\partial^3 w}{\partial x^3}\right) + \frac{1}{2}\left(\frac{\partial M_T}{\partial x}\right) = -\rho I\left(\frac{\partial^2 \Theta_x}{\partial t^2}\right) \tag{5.2.16}$$

$$\delta w : (-\mu A)\left[\left(\frac{\partial \Theta_x}{\partial x}\right) + \left(\frac{\partial^2 w}{\partial x^2}\right) + \left(\frac{l^2}{4}\right)\left(\frac{\partial^3 \Theta_x}{\partial x^3} - \frac{\partial^4 w}{\partial x^4}\right)\right] = -\rho A\left(\frac{\partial^2 w}{\partial t^2}\right) + f\left(x,t\right) \tag{5.2.17}$$

Also, at the end edges $x = 0$ and $x = L$ of the microbeam, the boundary conditions become

$$(EA)\left(\frac{\partial u}{\partial x}\right) - \frac{N_T}{2} = \widetilde{N}, \quad or \quad \delta u = 0 \tag{5.2.18}$$

$$\left[(EI) + \left(\frac{\mu A l^2}{4}\right)\right]\left(\frac{\partial \Theta_x}{\partial x}\right) - \left(\frac{\mu A l^2}{4}\right)\left(\frac{\partial^2 w}{\partial x^2}\right) - \left(\frac{M_T}{2}\right) = \widetilde{M} + \widetilde{M_h}, \quad or \quad \delta\Theta_x = 0 \tag{5.2.19}$$

$$(\mu A)\left[\Theta_x + \frac{\partial w}{\partial x} + \left(\frac{l^2}{4}\right)\left(\frac{\partial^2 \Theta_x}{\partial x^2} - \frac{\partial^3 w}{\partial x^3}\right)\right] = \widetilde{V}, \quad or \quad \delta w = 0 \tag{5.2.20}$$

$$\left(\frac{\mu A l^2}{4}\right)\left(\frac{\partial^2 w}{\partial x^2} - \frac{\partial \Theta_x}{\partial x}\right) = -\widetilde{V_h}, \quad or \quad \delta\left(\frac{\partial w}{\partial x}\right) = 0 \tag{5.2.21}$$

5.2.2 The DPL heat conduction model

The equation of non-Fourier heat conduction with a dual-phase-lagging effect involving the thermoelastic coupling is given by (Tzou, 2014) as

$$k\left(1 + \tau_T \frac{\partial}{\partial t}\right)\theta_{,ii} = \rho C_v \frac{\partial \theta}{\partial t} + T_0 \beta \frac{\partial u_{i,i}}{\partial t} + \rho C_v \tau_q \frac{\partial^2 \theta}{\partial t^2} + T_0 \tau_q \beta \frac{\partial^2 u_{i,i}}{\partial t^2} \tag{5.2.22}$$

In special case, if $\tau_T = 0$ and $\tau_q = 0$, the above model reduces to the classical Fourier heat conduction.

Using Eq. (5.2.1) into Eq. (5.2.22) provides the equation of thermal conduction as follows:

$$k\left(1+\tau_T\frac{\partial}{\partial t}\right)\left(\frac{\partial^2\theta}{\partial x^2}+\frac{\partial^2\theta}{\partial z^2}\right)=\rho C_v\left(\frac{\partial\theta}{\partial t}+\tau_q\frac{\partial^2\theta}{\partial t^2}\right)+T_0\beta\left(\frac{\partial^2 u}{\partial t\partial x}+z\frac{\partial^2\Theta_x}{\partial t\partial x}\right)+T_0\tau_q\beta\left(\frac{\partial^3 u}{\partial t^2\partial x}+z\frac{\partial^3\Theta_x}{\partial t^2\partial x}\right) \tag{5.2.23}$$

Multiplying both sides of above equation by $b\beta z$ and integrating with respect to the microbeam's thickness z from the range $-h/2$ to $+h/2$, gives

$$k\left(1+\tau_T\frac{\partial}{\partial t}\right)\left(\frac{\partial^2 M_T}{\partial x^2}+b\beta\int_{-h/2}^{+h/2}z\frac{\partial^2\theta}{\partial z^2}dz\right)=\rho C_v\left(\frac{\partial M_T}{\partial t}+\tau_q\frac{\partial M_T^2}{\partial t^2}\right)+T_0\beta^2 I\left(\frac{\partial^2\Theta_x}{\partial t\partial x}+\tau_q\frac{\partial^3\Theta_x}{\partial t^2\partial x}\right) \tag{5.2.24}$$

Substituting Eq. (3.1.11) into Eq. (5.2.24), it follows

$$k\left(1+\tau_T\frac{\partial}{\partial t}\right)\left(\frac{\partial^2 M_T}{\partial x^2}-P^2M_T\right)-\rho C_v\left(\frac{\partial M_T}{\partial t}+\tau_q\frac{\partial M_T^2}{\partial t^2}\right)=T_0\beta^2 I\left(\frac{\partial^2\Theta_x}{\partial t\partial x}+\tau_q\frac{\partial^3\Theta_x}{\partial t^2\partial x}\right) \tag{5.2.25}$$

The coupled thermoelastic governing equations considering the effects of MCST and DPL heat conduction model are derived as:

$$\delta u:-E\left(\frac{\partial^2 u}{\partial x^2}\right)=-\rho\left(\frac{\partial^2 u}{\partial t^2}\right)+\frac{G\left(x,t\right)}{A} \tag{5.2.26}$$

$$\delta\Theta_x:-\widetilde{H}\left(\frac{\partial^2\Theta_x}{\partial x^2}\right)+\left(\frac{\mu}{\iota_x^2}\right)\left(\Theta_x+\frac{\partial w}{\partial x}\right)+\left(\frac{\mu}{4}\right)\left(\frac{l}{\iota_x}\right)^2\left(\frac{\partial^3 w}{\partial x^2}\right)+\frac{1}{2I}\left(\frac{\partial M_T}{\partial x}\right)=-\rho\left(\frac{\partial^2\Theta_x}{\partial t^2}\right) \tag{5.2.27}$$

$$\partial w:-\mu\left[\left(\frac{\partial\Theta_x}{\partial x}\right)+\left(\frac{\partial^2 w}{\partial x^2}\right)+\left(\frac{l^2}{4}\right)\left(\frac{\partial^3\Theta_x}{\partial x^3}-\frac{\partial^4 w}{\partial x^4}\right)\right]=-\rho\left(\frac{\partial^2 w}{\partial t^2}\right)+\frac{f\left(x,t\right)}{A} \tag{5.2.28}$$

$$k\left(1+\tau_T\frac{\partial}{\partial t}\right)\left(\frac{\partial^2 M_T}{\partial x^2}-P^2M_T\right)-\rho C_v\left(\frac{\partial M_T}{\partial t}+\tau_q\frac{\partial M_T^2}{\partial t^2}\right)=T_0\beta^2 I\left(\frac{\partial^2\Theta_x}{\partial t\partial x}+\tau_q\frac{\partial^3\Theta_x}{\partial t^2\partial x}\right) \tag{5.2.29}$$

where $\widetilde{H} = E + \left(\frac{\mu}{4}\right)\left(\frac{l}{\iota_x}\right)^2$ in which $\iota_x = \sqrt{\frac{I}{A}} = \frac{h}{\sqrt{12}}$ is the cross-sectional radius of gyration passing through the center about y-axis.

Also, at edges $x = 0$ and $x = L$, the boundary conditions take the form

$$E\left(\frac{\partial u}{\partial x}\right) = \frac{\widetilde{N}}{A}, \quad or \quad \delta u = 0 \tag{5.2.30}$$

$$\widetilde{H}\left(\frac{\partial \Theta_x}{\partial x}\right) - \left(\frac{\mu}{4}\right)\left(\frac{l}{\iota_x}\right)^2\left(\frac{\partial^2 w}{\partial x^2}\right) - \frac{M_T}{2I} = \frac{\widetilde{M} + \widetilde{M_h}}{I}, \quad or \quad \delta\Theta_x = 0 \tag{5.2.31}$$

$$\mu\left[\left(\Theta_x + \frac{\partial w}{\partial x}\right) + \left(\frac{l^2}{4}\right)\left(\frac{\partial^2 \Theta_x}{\partial x^2} - \frac{\partial^3 w}{\partial x^3}\right)\right] = \frac{\widetilde{V}}{A}, \quad or \quad \delta w = 0 \tag{5.2.32}$$

$$\left(\frac{\mu l^2}{2}\right)\left(\frac{\partial^2 w}{\partial x^2} - \frac{\partial \Theta_x}{\partial x}\right) = -\frac{\widetilde{V_h}}{A}, \quad or \quad \delta\left(\frac{\partial w}{\partial x}\right) = 0 \tag{5.2.33}$$

For normalizing the governing equations and related boundary conditions, we define the following parameters in dimensionless form as follows:

$$\zeta = \frac{x}{L},\ \tau = \frac{t\varepsilon}{L},\ \varepsilon = \sqrt{\frac{E}{\rho}},\ \Theta = \Theta_x,\ \widetilde{u} = \frac{u}{h},\ \phi = \frac{w}{h},\ \psi = \frac{M_T}{EAh},\ \tau_1 = \frac{\tau_q \varepsilon}{L},\ \tau_2 = \frac{\tau_T \varepsilon}{L} \tag{5.2.34}$$

where, $\widetilde{u}$ and Θ are the non-dimensional values of in-plane deflection and rotational angle, respectively.

In view of Eq. (5.2.34), the normalized form of governing equations become

$$\delta\widetilde{u} : -\left(\frac{\partial^2 \widetilde{u}}{\partial \zeta^2}\right) = -\left(\frac{\partial^2 \widetilde{u}}{\partial \tau^2}\right) + G^* \tag{5.2.35}$$

$$\delta\Theta : -R_1\left(\frac{\partial^2 \Theta}{\partial \zeta^2}\right) + R_2\Theta - R_3\left(\frac{\partial^3 \phi}{\partial \zeta^3}\right) + R_4\left(\frac{\partial \phi}{\partial \zeta}\right) + R_5\left(\frac{\partial \psi}{\partial \zeta}\right) = -\left(\frac{\partial^2 \Theta}{\partial \tau^2}\right) \tag{5.2.36}$$

$$\delta\phi : R_6\left(\frac{\partial^3 \Theta}{\partial \zeta^3}\right) - R_7\left(\frac{\partial \Theta}{\partial \zeta}\right) + R_8\left(\frac{\partial^4 \phi}{\partial \zeta^4}\right) - R_9\left(\frac{\partial^2 \phi}{\partial \zeta^2}\right) = -\left(\frac{\partial^2 \phi}{\partial \tau^2}\right) + f^* \tag{5.2.37}$$

$$\left(1 + \tau_2\frac{\partial}{\partial t}\right)\left(\frac{\partial^2 \psi}{\partial \zeta^2} - R_{10}\psi\right) - R_{11}\left(\frac{\partial \psi}{\partial \tau}\right) - R_{12}\left(\frac{\partial^2 \psi}{\partial \tau^2}\right) = R_{13}\left(\frac{\partial^2 \Theta}{\partial \tau \partial \zeta}\right) + R_{14}\left(\frac{\partial^3 \Theta}{\partial \tau^2 \partial \zeta}\right) \tag{5.2.38}$$

where $G^* = \frac{G(x,t)}{\frac{EAh}{L^2}}$ and $f^* = \frac{f(x,t)}{\frac{EAh}{L^2}}$.

The coefficients used in the above calculations are shown in the Appendix.

It is assumed that the supports have no deflection and resistance against in-plane moment of particles on an edge in the normal direction. It is further assumed that on the edges of the microbeam there is no higher order stress as applied by the supports. Thus, the boundary conditions at $\zeta = 0$ and $\zeta = 1$ give

$$\begin{aligned} \widetilde{u} =& \frac{\partial^2 \widetilde{u}}{\partial \zeta^2} = 0,\ R_1 \left(\frac{\partial \Theta}{\partial \zeta} \right) + R_3 \left(\frac{\partial^2 \phi}{\partial \zeta^2} \right) - R_5 \left(\psi \right) = \frac{\partial \Theta}{\partial \zeta} = 0 \\ \phi =& R_6 \left(\frac{\partial \Theta}{\partial \zeta} \right) + R_8 \left(\frac{\partial^2 \phi}{\partial \zeta^2} \right) = \psi = 0 \end{aligned} \tag{5.2.39}$$

And the initial conditions at time $\tau = 0$ can be assumed as follows:

$$\widetilde{u} = \frac{\partial \widetilde{u}}{\partial \tau} = 0,\ \Theta = \frac{\partial \Theta}{\partial \tau} = 0,\ \phi = \frac{\partial \phi}{\partial \tau} = 0,\ \psi = \frac{\partial \psi}{\partial \tau} = 0 \tag{5.2.40}$$

We consider that the microbeam, kept at constant temperature, with simply supported ends is subjected to a constant force per unit length i.e. $f\left(x,t\right) = f_0 \delta\left(t\right)$. It is further assumed that there is no axial body force $G\left(x,t\right)$. In this case, the coupled thermoelastic governing equations are converted to

$$\delta \widetilde{u} : \left(\frac{\partial^2 \widetilde{u}}{\partial \zeta^2} \right) = \left(\frac{\partial^2 \widetilde{u}}{\partial \tau^2} \right) \tag{5.2.41}$$

$$\delta \Theta : -R_1 \left(\frac{\partial^2 \Theta}{\partial \zeta^2} \right) + R_2 \Theta - R_3 \left(\frac{\partial^3 \phi}{\partial \zeta^3} \right) + R_4 \left(\frac{\partial \phi}{\partial \zeta} \right) + R_5 \left(\frac{\partial \psi}{\partial \zeta} \right) = - \left(\frac{\partial^2 \Theta}{\partial \tau^2} \right) \tag{5.2.42}$$

$$\delta \phi : R_6 \left(\frac{\partial^3 \Theta}{\partial \zeta^3} \right) - R_7 \left(\frac{\partial \Theta}{\partial \zeta} \right) + R_8 \left(\frac{\partial^4 \phi}{\partial \zeta^4} \right) - R_9 \left(\frac{\partial^2 \phi}{\partial \zeta^2} \right) = - \left(\frac{\partial^2 \phi}{\partial \tau^2} \right) + f_0^* \delta\left(t\right) \tag{5.2.43}$$

$$\left(1+\tau_2\frac{\partial}{\partial t}\right)\left(\frac{\partial^2\psi}{\partial\zeta^2}-R_{10}\psi\right)-R_{11}\left(\frac{\partial\psi}{\partial\tau}\right)-R_{12}\left(\frac{\partial^2\psi}{\partial\tau^2}\right)=R_{13}\left(\frac{\partial^2\Theta}{\partial\tau\partial\zeta}\right)+R_{14}\left(\frac{\partial^3\Theta}{\partial\tau^2\partial\zeta}\right) \tag{5.2.44}$$

where $f_0^*=\frac{f_0}{\frac{EAh}{L^2}}$.

5.3 Solution of the problem

In order to solve the governing equations (5.2.42)-(5.2.44), we adopt the Laplace transform technique. Applying the Laplace transform to both sides of Eqs. (5.2.42)-(5.2.44) and using the initial conditions (50), we arrive at the following relations:

$$-R_1\left(\frac{\partial^2\overline{\Theta}}{\partial\zeta^2}\right)+\left(R_2+s^2\right)\overline{\Theta}-R_3\left(\frac{\partial^3\overline{\phi}}{\partial\zeta^3}\right)+R_4\left(\frac{\partial\overline{\phi}}{\partial\zeta}\right)+R_5\left(\frac{\partial\overline{\psi}}{\partial\zeta}\right)=0 \tag{5.3.1}$$

$$R_6\left(\frac{\partial^3\overline{\Theta}}{\partial\zeta^3}\right)-R_7\left(\frac{\partial\overline{\Theta}}{\partial\zeta}\right)+R_8\left(\frac{\partial^4\overline{\phi}}{\partial\zeta^4}\right)-R_9\left(\frac{\partial^2\overline{\phi}}{\partial\zeta^2}\right)+s^2\overline{\phi}=f_0^* \tag{5.3.2}$$

$$(1+\tau_2 s)\left(\frac{\partial^2\overline{\psi}}{\partial\zeta^2}\right)-\left[R_{10}+\left(\tau_2 R_{10}+R_{11}\right)s+R_{12}s^2\right]\overline{\psi}=\left(R_{13}s+R_{14}s^2\right)\left(\frac{\partial\overline{\Theta}}{\partial\zeta}\right) \tag{5.3.3}$$

where $\overline{\Theta}$ denote the Laplace transform of Θ and s represents the parameter of Laplace transform.

Following the Fourier series method to solve the governing equations (5.3.1)-(5.3.3) with all the boundary conditions given in Eq. (5.2.39), the solutions are taken as follows:

$$\left.\begin{aligned}\overline{\Theta}(\zeta,s)&=\sum_{m=0}^{\infty}\overline{\Theta}_m(s)\,cos\,(r_m\zeta)\\ \overline{\phi}(\zeta,s)&=\sum_{m=1}^{\infty}\overline{\phi}_m(s)\,sin\,(r_m\zeta)\\ \overline{\psi}(\zeta,s)&=\sum_{m=1}^{\infty}\overline{\psi}_m(s)\,sin\,(r_m\zeta)\end{aligned}\right\} \tag{5.3.4}$$

And the constant normalized force f_0^* per unit length is given by

$$f_0^* = \sum_{m=0}^{\infty} Q_m sin\left(r_m \zeta\right) \tag{5.3.5}$$

where

$$Q_m = 2\int_0^1 f_0^* sin\left(r_m \zeta\right) d\zeta = \frac{4f_0^*}{r_m} \tag{5.3.6}$$

The term $\overline{\Theta}_m$ indicates the Fourier transform of $\overline{\Theta}$.

Inserting Eqs. (5.3.5) and (5.3.6) into Eqs. (5.3.1)-(5.3.3), we obtain

$$\left(R_1 r_m^2 + R_2 + s^2\right)\overline{\Theta}_m + \left(R_3 r_m^3 + R_4 r_m\right)\overline{\phi}_m + \left(R_5 r_m\right)\overline{\psi}_m = 0 \tag{5.3.7}$$

$$-\left(R_6 r_m^3 + R_7 r_m\right)\overline{\Theta}_m + \left(R_8 r_m^4 + R_9 r_m^2 + s^2\right)\overline{\phi}_m = Q_m \tag{5.3.8}$$

$$\left[\left(r_m^2 + R_{10}\right) + \left(\tau_2 r_m^2 + \tau_2 R_{10} + R_{11}\right)s + R_{12}s^2\right]\overline{\psi}_n + \left(R_{13} r_m s + R_{14} r_m s^2\right)\overline{\Theta}_m = 0 \tag{5.3.9}$$

Thus, the solution for normalized deflection can be obtained as:

$$\overline{\phi}_m\left(s\right) = Q_m \frac{w_0 + w_1 s + w_2 s^2 + w_3 s^3 + w_4 s^4}{\overline{w}_0 + \overline{w}_1 s + \overline{w}_2 s^2 + \overline{w}_3 s^3 + \overline{w}_4 s^4 + \overline{w}_5 s^5 + \overline{w}_6 s^6} \tag{5.3.10}$$

The coefficients of above equation are shown in the Appendix.

Now, by taking the inversion of Laplace transform of Eq. (5.3.10) provides the solution for normalized deflection as follows:

$$\phi_m\left(\tau\right) = Q_m \sum_{i=1}^{6}\left(\frac{w_0 + w_1\alpha_i + w_2\alpha_i^2 + w_3\alpha_i^3 + w_4\alpha_i^4}{\overline{w}_1 + 2\overline{w}_2\alpha_i + 3\overline{w}_3\alpha_i^2 + 4\overline{w}_4\alpha_i^3 + 5\overline{w}_5\alpha_i^4 + 6\overline{w}_6\alpha_i^5}\right)e^{(\alpha_i \tau)} \tag{5.3.11}$$

where α_i denotes the all six roots of the equation $\overline{w}_0 + \overline{w}_1\alpha + \overline{w}_2\alpha^2 + \overline{w}_3\alpha + \overline{w}_4\alpha^4 + \overline{w}_5\alpha^5 + \overline{w}_6\alpha^6 = 0$. In view of Eq. (5.3.5), the desired normalized deflection is derived

as:

$$\phi(\zeta,\tau) = \sum_{m=1,3,..}^{\infty} \phi_m(\tau)\, sin(r_m\zeta)$$
$$= \sum_{m=1,3,..}^{\infty} Q_m \sum_{i=1}^{6} \left(\frac{w_0 + w_1\alpha_i + w_2\alpha_i^2 + w_3\alpha_i^3 + w_4\alpha_i^4}{\overline{w}_1 + 2\overline{w}_2\alpha_i + 3\overline{w}_3\alpha_i^2 + 4\overline{w}_4\alpha_i^3 + 5\overline{w}_5\alpha_i^4 + 6\overline{w}_6\alpha_i^5} \right) e^{(\alpha_i\tau)} sin(r_m\zeta) \tag{5.3.12}$$

In a similar way, the normalized midspan thermal moment of the microbeam can be derived as:

$$\psi(\zeta,\tau) = \sum_{m=1,3,..}^{\infty} \psi_m(\tau)\, sin(r_m\zeta)$$
$$= \sum_{m=1,3,..}^{\infty} Q_m \sum_{i=1}^{6} \left(\frac{\widetilde{w}_1\alpha_i + \widetilde{w}_2\alpha_i^2}{\overline{w}_1 + 2\overline{w}_2\alpha_i + 3\overline{w}_3\alpha_i^2 + 4\overline{w}_4\alpha_i^3 + 5\overline{w}_5\alpha_i^4 + 6\overline{w}_6\alpha_i^5} \right) e^{(\alpha_i\tau)} sin(r_m\zeta) \tag{5.3.13}$$

In the Appendix, the coefficients for above equation are given. This completes the analytical solution of the present problem.

5.4 Results and discussion

In the previous section, the explicit expressions for normalized deflection and normalized thermal moment of a Timoshenko microbeam has been developed considering the effects of MCST and DPL heat conduction model. Now, in order to illustrate the results, we carry out numerical computation. The results under DPL, LS, and Fourier heat conduction models are separately obtained and compared in the context of MCST. The comparison between classical theory and the MCST for DPL heat conduction model is also investigated. Furthermore, the effects of phase-lags on the normalized deflection and thermal moment are also examined.

In the simulation, the beam is considered to be made of Silicon material. The reference temperature is set as $T_0 = 293\,K$. Thus, at this particular reference temperature, the known values of parameters of Silicon material are given as below (Taati et al., 2014)

$E = 169\,GPa$, $\rho = 2330\,kg/m^3$, $C_v = 713\,J/kgK$, $\alpha_T = 2.59 \times 10^{-6} 1/K$, $\nu = 0.22$, and $k = 156\,W/mK$.

There is lack of experimental data for the values of phase-lags time τ_q and τ_T. However, a fixed range from $10\,s$ to $50\,s$ have been given for some materials (Lopez et al., 2009; Shih et al., 2005). Following this, the results of the present work are obtained by setting the hypothetical values of phase-lags as $\tau_q = 16\,s$ and $\tau_T = 12\,s$ except where the effects of phase-lags are analyzed. Moreover, the aspect ratios of length to height and width to height of microbeam are set to be $L/h = 10$ and $b/h = 0.5$, respectively, except where these effects are shown. In this work, one more assumption taking into account that q is equal to EAh/L^2, therefore $f_0^* = 1$ (Taati et al., 2014). Results are shown in different figures.

Fig. 5.4.1 describes the variation of the normalized midspan deflection of the microbeam under classical theory ($l = 0$) and MCST in the context of the DPL thermoelastic model. The aspect ratio of length-scale parameter and microbeam thickness is fixed here as $l/h = 0.3$. It is observed that the peak values predicted by classical theory is higher than the peak values predicted by MCST and the peak values under classical theory are attained at a later time as compared to the MCST. Under these two theories, the variations of normalized midspan deflection are nearly the same for a small time range. However, the phase-difference between these two models increases simultaneously with the increases of time. Moreover, the deflection response of Timoshenko beam modeled by MCST indicates more energy dissipation as compared to the classical theory.

The comparison among the predictions of the normalized midspan deflection by

Lord-Shulman (LS), dual-phase-lag (DPL), and Fourier heat conduction models is shown in Figure 5.4.2 for a particular aspect ratio $l/h = 0.3$. It is revealed from Fig. 5.4.2 that at smaller range of time, there is a good agreement under these three models, but the plots under DPL and LS models diverge from the plot by Fourier heat conduction model as time increases. Hence, the difference of peak values increases. It is noticed that the phase-difference of deflection between DPL and LS models are approximately the same while the difference in peak values increases rapidly as time increases. Moreover, the peak values are attained much earlier in case of Fourier model as compared to the generalized models, i.e., LS and DPL models and this disagreement of models is pronounced significantly at higher time.

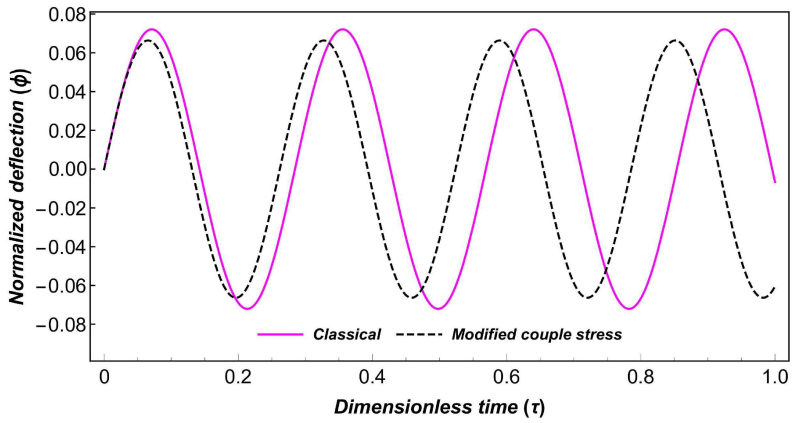

Figure 5.4.1: Response of normalized midspan deflection of microbeam w.r.t. dimensionless time considering classical theory and MCST for fixed $l/h = 0.3$.

Fig. 5.4.3 reveals the vibration response of normalized midspan thermal moment against dimensionless time in the contexts of classical theory and MCST for fixed dimensionless aspect ratio $l/h = 0.3$. It is observed that at the beginning, the variation of thermal moment is approximately the same under both classical theory and MCST the-

ories, but the phase-difference between these models is more prominent as dimensionless time increases. It is further observed that frequency response of thermal moment under MCST is much faster than classical theory which offers more energy dissipation during vibrations. Hence, the oscillations under MCST will occur for a small time as compared to the oscillations under classical theory.

The difference between response of the normalized midspan thermal moment under LS, DPL, and Fourier heat conduction models has been illustrated in Figure 5.4.4 in the case of the MCST. Here, the aspect ratio of material length-scale parameter and thickness of the microbeam is considered to be $l/h = 0.3$. From the Figure, the inference can be drawn that the vibrations of thermal moment under Fourier heat conduction model indicates the high energy dissipation than LS and DPL models. In the starting, the response of thermal moment under LS and DPL models shows a good agreement when the dimensionless time is kept less than 5, while the frequency response of these two models diverges when the dimensionless time increases beyond 5. It is further noticed that the phase difference of thermal moment between these three models increases with the increase of time.

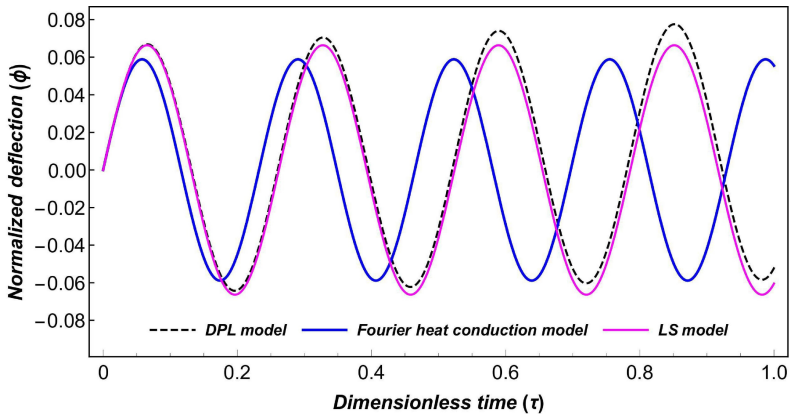

Figure 5.4.2: Response of normalized midspan deflection of microbeam w.r.t. dimensionless time considering MCST for LS, DPL, and Fourier heat conduction models for fixed $l/h = 0.3$.

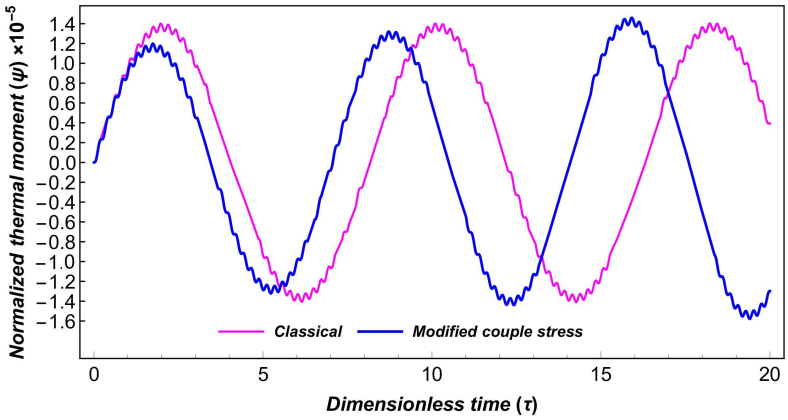

Figure 5.4.3: Response of normalized midspan thermal moment of microbeam w.r.t. dimensionless time considering classical theory and MCST for fixed $l/h = 0.3$.

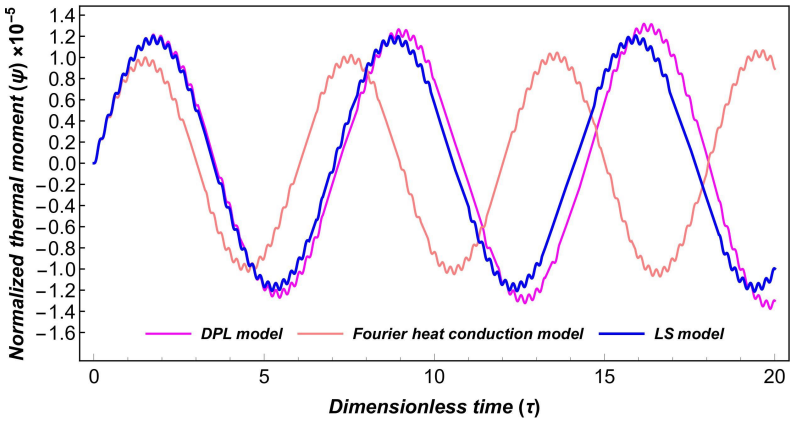

Figure 5.4.4: Response of normalized midspan thermal moment of microbeam w.r.t. dimensionless time considering MCST for LS, DPL, and Fourier heat conduction models for fixed $l/h = 0.3$.

Fig. 5.4.5 depicts the effects of length-scale parameter on the time variation of normalized midspan deflection of microbeam by employing DPL model. The obtained results are plotted for different aspect ratios of length-scale parameter and the thickness of the microbeam l/h, i.e ($l/h = 0$, 0.4, 1). It can be seen that the frequency responses

of deflection are more significant when aspect ratio l/h increases. Thus, it is apparent that more energy dissipation can occur as length-scale parameter increases.

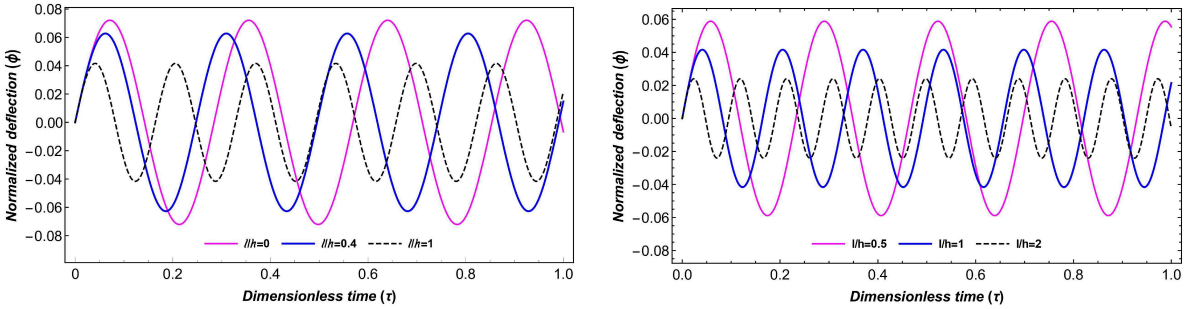

Figure 5.4.5: Response of normalized midspan deflection of microbeam w.r.t. dimensionless time considering MCST for varying aspect ratios (a) $l/h(l/h = 0, 0.4, 1)$ and (b) $l/h(l/h = 0.5, 1, 2)$.

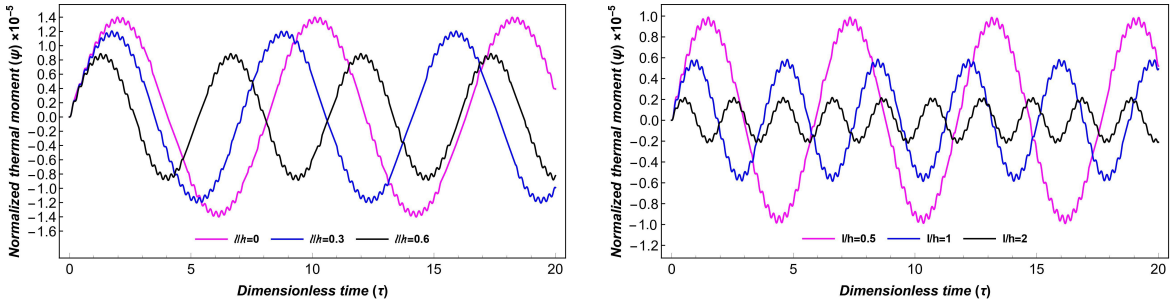

Figure 5.4.6: Response of normalized midspan thermal moment of microbeam w.r.t. dimensionless time considering MCST for varying aspect ratios (a) $l/h(l/h = 0, 0.3, 0.6)$ and (b) $l/h(l/h = 0, 5, 1, 2)$.

The effects of the aspect ratio of length-scale parameter and thickness of the microbeam on the normalized midspan thermal moment is shown in Figure 5.4.6. It is observed that the phase-difference of variation of thermal moment is more significant when l/h increases. Thus, the length-scale parameter shows strong influence on the variation of microbeam's thermal moment.

Fig. 5.4.7 displays the variation of the normalized midspan deflection versus dimensionless time for several aspect ratios L/h ($L/h = 4,\ 6,\ 10$) when the aspect ratio l/h is set to the value $l/h = 0.3$. According to the Figure, the phase difference of deflection decreases as the aspect ratio L/h becomes larger by indicating the higher peaks in a specific time interval. The same fact has been stated by Taati et al. (2014) for strain gradient theory.

The variation of normalized midspan thermal moment of microbeam against dimensionless time is shown in Figure 5.4.8 for several values of aspect ratios L/h ($L/h = 4,\ 6,\ 10$). The dimensionless aspect ratio l/h is set again here as (a) $l/h = 0$, (b) $l/h = 0.3$, (c) $l/h = 0.6$. It is revealed here that the phase-difference of thermal moment is enhanced and the peak value at a specific interval decreases when L/h increases. It is further observed that higher value of L/h minimizes the energy dissipation of thermal moment which is compatible for more oscillations in the system. Also, the large value of aspect ratio l/h offers more energy dissipation with an increase in the peak value. This implies that the oscillations will happen for a short duration of time.

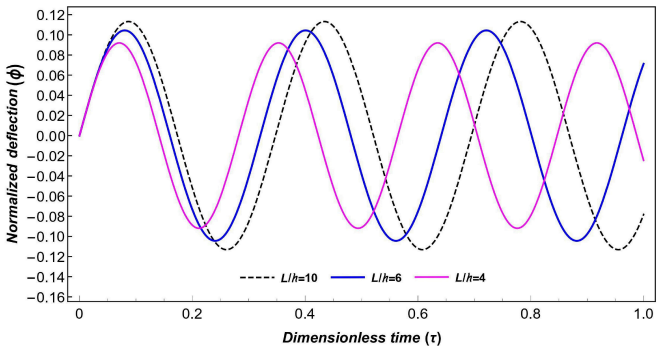

Figure 5.4.7: Response of normalized midspan deflection of microbeam w.r.t. dimensionless time considering MCST for varying aspect ratio $L/h(L/h = 4,\ 6,\ 10)$ and for fixed $l/h = 0.3$.

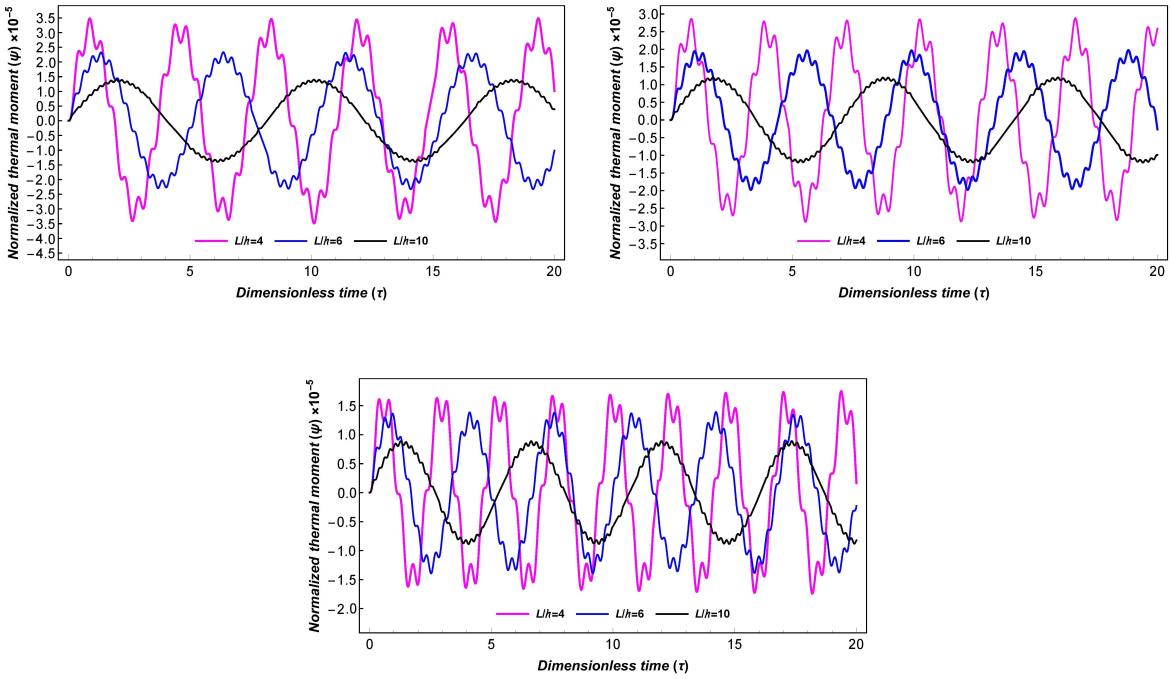

Figure 5.4.8: Response of normalized midspan thermal moment of microbeam w.r.t. dimensionless time considering MCST for varying aspect ratio $L/h(L/h = 4, 6, 10)$ and for fixed (a) $l/h = 0$, (b) $l/h = 0.3$, (c) $l/h = 0.6$.

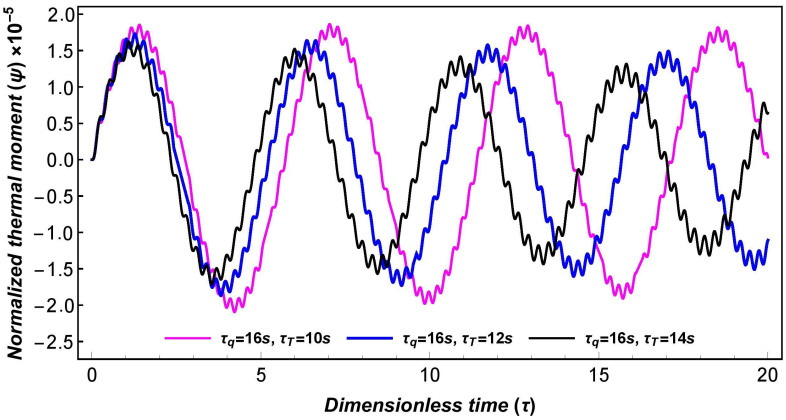

Figure 5.4.9: Effect of phase-lags on the normalized midspan thermal moment of microbeam w.r.t. dimensionless time considering MCST for fixed $l/h = 0.3$.

Fig. 5.4.9 illustrates the effects of the phase-lags under DPL heat conduction model on the time variation of thermal moment for a fixed $l/h = 0.3$. According to these

Figures, the frequencies of thermal moment are shifted and also the phase-difference increases with the increase in phase-lags time parameter. It is worth noting that the response of thermal moment are more faster for higher values of phase-lags time parameters. This clears that for small phase-lag times, the oscillations will remain for a longer time.

5.5 Conclusion

The present work involves the study of dynamic behavior of a Timoshenko microbeam considering MCST and DPL thermoelastic model. The normalized form of midspan deflection and thermal moment of a Timoshenko microbeam are constructed. The governing equations and related boundary conditions of microbeam are derived by employing the Hamilton's principle. A detailed comparison among the predictions by different heat conduction theories like, DPL, LS, and Fourier heat conduction theories is explored. The present study also validates the comparison between classical and MCST for the DPL heat conduction model. The major conclusions of the present work can be made as follows:

- There are strong influences of two phase-lags on the variation of the normalized midspan thermal moment when the DPL heat conduction model is taken into account.

- For small time range, the responses of thermal moment and deflection under DPL, LS, and Fourier heat conduction models converge and diverge from each other for large time range.

- The classical elasticity theory offers a lower rate of energy dissipation as compared to MCST in the context of DPL heat conduction.

- The frequency response becomes more faster when length-scale parameter in-

creases.

- The frequency response under LS and Fourier thermoelastic models is faster than DPL model leading to more energy dissipation.
- The phase-difference of deflection and thermal moment decreases with an increase in the length of the microbeam.
- The size-effects on the frequency response are observed prominently when the DPL model is employed.